All-optical Ti:PPLN wavelength conversion modules for free-space optical transmission links in the mid-infrared

Kai-Daniel F. Büchter,[1,*] Harald Herrmann,[1] Carsten Langrock,[2] Martin M. Fejer,[2] and Wolfgang Sohler[1]

[1]*Angewandte Physik, Universität Paderborn, Warburger Strasse 100, 33098 Paderborn, Germany*
[2]*Edward L. Ginzton Laboratory, Stanford University, Stanford, California 94305, USA*
**Corresponding author: sol_db@physik.uni-paderborn.de*

Received August 8, 2008; revised October 26, 2008; accepted December 12, 2008;
posted January 12, 2009 (Doc. ID 100253); published February 10, 2009

Data-format-independent all-optical transmitter and receiver modules for free-space optical communications in the 3.8 μm region have been developed, essentially consisting of Ti-indiffused, periodically poled $LiNbO_3$ waveguides. Using these modules, conversion of *C*-band radiation to/from the mid-infrared (MIR) via difference-frequency generation was demonstrated. More than 10 mW of MIR power could be generated with the transmitter unit; the internal low-power conversion efficiency was 69%/W. A free-space MIR link was set up with a −41 dB fiber-to-fiber loss; only −15 dB are due to the parametric processes.

OCIS codes: 060.2605, 070.4340, 130.3060, 130.7405.

In free-space optical (FSO) data transmission the use of mid-infrared (MIR) radiation can be advantageous over *C*-band radiation, since scattering and scintillation effects decrease with increasing wavelength [1]. In addition, an atmospheric transmission window can be found around 3.8 μm [2]. Therefore, devices that enable all-optical wavelength conversion between *C*-band and MIR radiation are highly desirable for data-format-independent and secure FSO links. We developed integrated optical transmitter and receiver modules exploiting difference-frequency generation (DFG) in Ti-indiffused waveguides in periodically poled $LiNbO_3$ (Ti:PPLN) and demonstrated their applicability in a MIR–FSO link experiment.

Several quasi-phase-matched PPLN waveguide devices for MIR generation have been developed and applied to absorption spectroscopy of trace gases [3–6]. With a pump source at $\lambda \approx 1$ μm and a signal source in the *C* band, DFG leads to the generation of MIR idler radiation. A MIR power of 65 mW at 3.4 μm generated in a directly bonded waveguide device was reported recently, at pump and signal powers of about 0.5 W each; the low-power efficiency of this device was 35%/W [7].

Ti:PPLN waveguides are an attractive alternative, promising low propagation losses over long interaction lengths. With such waveguides, *C*-band signals can be converted to the 3.8 μm range, if a pump source at $\lambda_{p.} = 1100$ nm is used and domain periods around 27 μm are chosen to obtain quasi-phase matching (QPM). While until now research has focused on the downconversion of near-infrared (NIR) signals to the MIR, we also demonstrate the consecutive step of regenerating a NIR (*C*-band) signal from the MIR by upconversion to realize a FSO link.

Modeling based on coupled-mode equations was performed to optimize the DFG efficiency. In Fig. 1 the calculated MIR (idler) power is shown as a function of launched pump and signal powers assuming an 80-mm-long waveguide. The results reveal that at moderate pump and signal powers about 10 mW of MIR power can be generated. Hundreds of milliwatts of idler power can even be expected with pump and signal powers in the watt range.

Based on these encouraging results, two wavelength conversion modules were developed (Fig. 2). Their waveguides were fabricated by indiffusion of 18-μm-wide and 160-nm-thick titanium stripes for 31 h at 1060°C into a *Z*-cut $LiNbO_3$ crystal. After indiffusion, an 80-mm-long QPM grating with a periodicity of 26.65 μm was fabricated by electric-field-assisted poling. The typical propagation loss of such a waveguide was measured to be 0.05 dB/cm at 3.39 μm wavelength. At the fiber-coupled input, a 3-mm-long linear waveguide taper (from 4 to 18 μm width) facilitates the excitation of fundamental waveguide modes at pump and signal wavelengths. The end face at this side was polished under an angle of 5.3° to suppress interference effects within the waveguide as well as backreflections into the fiber. The opposite side was polished perpendicular to the waveguide axis to simplify free-space coupling to the transmission line. The 83-mm-long sample was housed in a temperature-stabilized oven that could

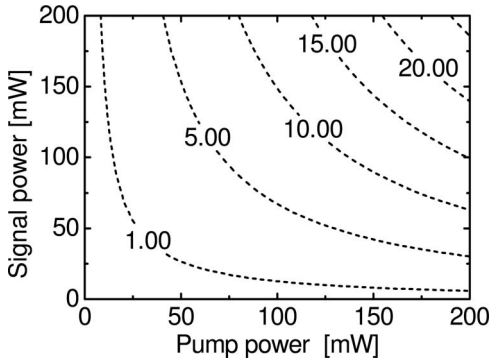

Fig. 1. Calculated MIR power in milliwatts generated by DFG in an 80-mm-long Ti-diffused PPLN waveguide as a function of coupled pump and signal power.

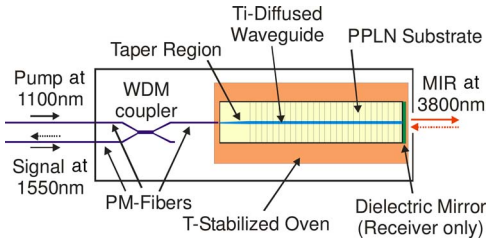

Fig. 2. (Color online) Schematic of the transmitter–receiver module. The receiver module has an additional dielectric mirror to enable copropagating DFG of MIR radiation and pump from right to left.

be heated to above 200 °C to avoid photorefraction. Pump and signal were combined by a polarization-maintaining (PM) fiber-WDM coupler and coupled to TM waveguide modes (exploiting the strong d_{33} coefficient), using an 8° angle polished ferrule. Owing to the high operating temperatures a micropositioner was used for coupling, instead of gluing the fiber to the sample. The outcoupled MIR radiation was collimated by an $f=8.3$ mm CaF_2 lens; a Ge filter was used to block residual NIR radiation in the free-space beam.

In the receiver module a dielectric mirror that reflects the pump and transmits the idler was deposited on the end face of the waveguide to enable codirectional DFG of pump and incoming 3.8 μm MIR radiation. The mirror consists of a stack of 12 Monte Carlo optimized SiO_2 and TiO_2 layers. Characterization on a witness sample confirmed a reflectivity of ~95% at 1.1 μm and high transmission (>97%) at 3.8 μm. The mirror allows the same fiber optics to be used in both modules, without the need for a 3.8/1.1 μm coupler at the free-space input. The regenerated 1.55 μm radiation is routed to the signal port by the WDM for detection.

Characterization of the two modules was done using an Yb-doped 1.1 μm fiber laser as the pump and a tunable external-cavity laser, followed by an erbium-doped fiber amplifier, as the signal source. QPM could be adjusted by tuning either the signal wavelength or the device temperature T. In Fig. 3, the measured phase-matching characteristics of both modules are shown (left, both modules operated as transmitter), along with calculated ones (right). The normalized idler power is given versus signal wavelength at $T=197$ °C. The maximum output power is achieved at a signal wavelength of $\lambda_s=1554.4$ nm, corresponding to an MIR wavelength of $\lambda_i=3764$ nm. In the ideal case, a sinc^2-type wavelength response is expected. However, strong sidelobes at the short wavelength side arise from waveguide inhomogeneities (variations in width, depth) and from negative temperature gradients toward the sample ends. These have been modeled by assuming a parabolic chirp of the phase mismatch $\Delta\beta$. Such inhomogeneities lead to a reduced peak efficiency, as the area enclosed under the phase-matching curves is nearly constant (the curves in Fig. 3 are normalized in this way). However, a potential transmission of data is unimpaired by sidelobes, as long as the signal bandwidth is significantly smaller than the phase-matching bandwidth. The phase-matching characteristics of both modules are very similar, but a shorter effective interaction length leads to a somewhat lower conversion efficiency and broader spectral response in the receiver module.

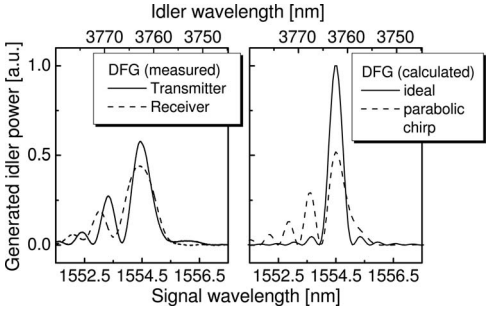

Fig. 3. Measured phase-matching characteristics of both modules (left) as well as calculated ones, with and without parabolic chirp of $\Delta\beta$ (right); all are normalized to the enclosed area. The chirp corresponds to a variation of either temperature $\Delta T \approx -13$ °C, Ti strip width $\Delta w \approx -1.6$ μm, Ti strip thickness $\Delta d \approx 5$ nm, or diffusion temperature $\Delta T_{\mathrm{diff}} \approx 2.3$ °C.

In Fig. 4, the measured MIR power from the transmitter module at $\lambda_s=1554.4$ nm is plotted versus the product of coupled pump and signal powers at the waveguide input. Power was determined by measurements in the free-space beam and subsequent correction for Fresnel losses, waveguide propagation losses, as well as residual losses in the Ge filter. In addition, calculated power characteristics, assuming $d_{33}=24$ pm/V, are shown (compare Fig. 1). The slopes of measured and calculated responses fit well at small power levels, although a smaller slope is expected for the experimental data owing to the non-ideal phase-matching characteristics (Fig. 3). We attribute this discrepancy to uncertainties of some experimental parameters, the nonlinear coefficient, and the waveguide model. At a fixed signal power of 50 mW, a linear increase of the idler power with pump power is observed with a power normalized conversion efficiency of 69%/W. This characteristic should become superlinear at higher pump levels owing to parametric amplification. At fixed pump power of 150 mW, a roll-off is observed at high signal power levels, which

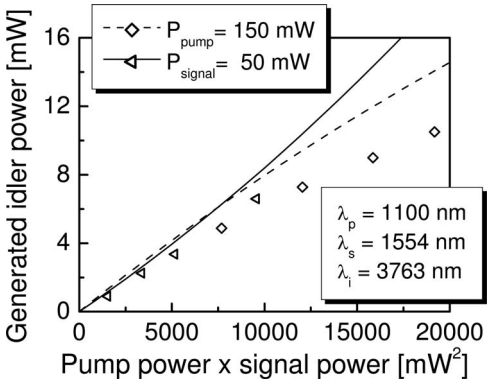

Fig. 4. Measured output power of the transmitter module (symbols), depending on pump and signal power levels coupled to the waveguide. The curves represent corresponding calculations.

is due to the onset of pump depletion. The maximum MIR power was 10.5 mW when 150 mW of pump and 130 mW of signal power were coupled to the waveguide, corresponding to a power conversion efficiency of 8%. Maximum input power was limited by the fiber optic WDM couplers.

Using both modules, a 1.5-m-long MIR–FSO link was set up, using two gold mirrors to couple radiation from the transmitter to the receiver (Fig. 5, left). Both modules were operated using a single pump laser followed by a 3 dB coupler. The wavelength dependence of the power regenerated by the receiver module is displayed in Fig. 5, right. The measured response agrees well with the product of transmitter and receiver phase-matching characteristics (see Fig. 3, left). At a MIR power level of 4.85 mW in the FSO link, generated by pump and signal powers of 150 and 80 mW, respectively, coupled to the transmitter waveguide, about 100 μW (25 μW) of signal power was regenerated in the receiver waveguide (measured at the fiber output). Therefore, the transmission for the signal equals −29 dB, of which −14 dB can be attributed to the MIR–FSO link (Fresnel losses, residual losses in the Ge filter, collimation and coupling losses). The remaining −15 dB are due to the parametric processes in the two wavelength converters. Fiber optic, Fresnel, and coupling losses from the signal source to the transmitter waveguide and equivalent losses from the receiver waveguide to the detector add −6 dB losses for each module, resulting in an overall fiber-to-fiber loss of −41 dB.

In conclusion, a *C*-band–MIR–*C*-band FSO link was set up, demonstrating the successful downconversion and upconversion of radiation in Ti:PPLN waveguides. There is a large potential for reducing the −14 dB losses in the MIR–FSO link by improved coupling using optimized, antireflection-coated lenses. By pumping with higher powers, the −15 dB losses of the conversion processes can be reduced, potentially leading to parametric gain. For example, a pump power of 850 mW coupled to each waveguide would reduce the conversion losses to 0 dB. This would require improved WDM couplers, possibly integrated on the $LiNbO_3$ substrate. Moreover, the additional −6 dB loss on the input and output sides can be reduced by improving fiber-to-waveguide coupling.

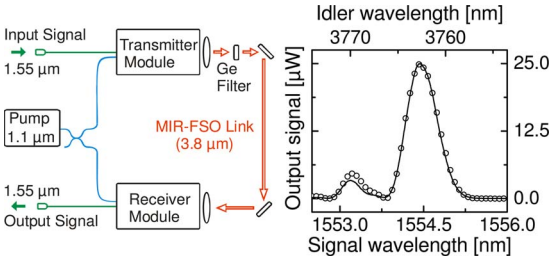

Fig. 5. (Color online) MIR–FSO link of 1.5 m length set up with transmitter and receiver modules (left). Measured (circles) and expected (solid curve) output signal power versus the signal wavelength (input signal power: 320 mW) (right).

Data transmission experiments via the link were done recently. Using quadrature phase shift keyed modulation at 2.488 Gbits/s, low bit error rates could be demonstrated [8]. The impact of parametric noise is negligible. At 150 mW power at 1.55 μm wavelength this noise is of the order of 1 nW within the phase-matching bandwidth of a comparable Ti:PPLN waveguide [9]. This means that the signal-to-noise ratio considerably exceeds 10^6. In addition, receiver modules could be operated as transceivers enabling bidirectional communication, using slightly different phase-matching wavelengths to avoid cross talk due to the nonlinear process.

This work was supported by a subcontract from CeLight, Inc.

References

1. R. Martini, C. Gmachl, J. Falciglia, F. G. Curti, C. G. Bethea, F. Capasso, E. A. Whittaker, R. Paiella, A. Tredicucci, A. L. Hutchinson, D. L. Sivco, and A. Y. Cho, Electron. Lett. **37**, 191 (2001).
2. W. A. Traub and M. T. Stier, Appl. Opt. **15**, 364 (1976).
3. K. P. Petrov, A. T. Ryan, T. L. Patterson, L. Huang, S. J. Field, and D. J. Bamford, Appl. Phys. B **67**, 357 (1998).
4. O. Tadanaga, T. Yanagawa, Y. Nishida, H. Miyazawa, K. Magari, M. Asobe, and H. Suzuki, Appl. Phys. Lett. **88**, 061101 (2006).
5. T. Yanagawa, O. Tadanaga, K. Magari, Y. Nishida, H. Miyazawa, M. Asobe, and H. Suzuki, Appl. Phys. Lett. **89**, 221115 (2006).
6. D. Richter, P. Weibring, A. Fried, O. Tadanaga, Y. Nishida, M. Asobe, and H. Suzuki, Opt. Express **15**, 564 (2007).
7. M. Asobe, O. Tadanaga, T. Yanagawa, T. Umeki, Y. Nishida, and H. Suzuki, Electron. Lett. **44**, 288 (2008).
8. E. Ip, D. Büchter, C. Langrock, J. M. Kahn, H. Herrmann, W. Sohler, and M. M. Fejer, in *Proceedings of the European Conference and Exhibition on Optical Communication* (IEEE, 2008), paper Tu.3.E.7.
9. S. Orlov, W. Grundkötter, D. Hofmann, V. Quiring, R. Ricken, H. Suche, and W. Sohler, in *Mid-Infrared Coherent Sources and Applications*, NATO Science Series—B: Physics and Biophysics, M. Ebrahimzadeh and I. T. Sorokina, eds. (Springer, 2008).